

A multiaxial stress-strain correction scheme

HOLGER LANG¹, KLAUS DRESSLER², RENE PINNAU³

^{1,2} Fraunhofer Institut für Techno- und Wirtschaftsmathematik,
Fraunhofer Platz 1, 67663 Kaiserslautern, Germany
holger.lang@itwm.fraunhofer.de, klaus.dressler@itwm.fraunhofer.de

³ Technische Universität Kaiserslautern,
Erwin Schrödinger Strasse, Geb. 48, 67663 Kaiserslautern, Germany
pinnau@mathematik.uni-kaiserslautern.de

Abstract

A method to correct the elastic stress tensor over time at a fixed point of an elastoplastic body, which is subject to exterior loads, is presented and mathematically analysed. In contrast to uniaxial corrections (Neuber or ESED), our method takes multiaxiality phenomena like cyclic hardening/softening, ratchetting and non-masing behaviour into account using Jiang's model of nonlinear elastoplasticity. Our numerical algorithm is designed for the case that the scalar loads are piecewise linear and can be used e.g. in connection with critical plane/multiaxial rainflow methods in high cycle fatigue analysis. In addition, a local existence and uniqueness result for a generalized solution of Jiang's system of discontinuous ordinary differential equations is given.

Keywords. Jiang's model, elastoplasticity, multiaxial high cycle fatigue analysis, durability, differential inclusions, Filippov theory, discontinuous ordinary differential equations

MSC classification: 74C15, 74D10, 65L06

1 Introduction

1.1 Motivation.

Let $U \subset \mathbb{R}^3$ be a domain, representing a homogeneous elastoplastic metallic body, that is subject to loads, and whose points $x \in \bar{U}$ undergo a nonlinear multiaxial constitutive material law of the form

$$\sigma(t, x) = \int_0^t C^{ep} \dot{\varepsilon}(\tau, x) d\tau, \quad (1)$$

where the elastoplastic tensors $C^{ep} \in \mathbb{R}^{3 \times 3 \times 3 \times 3}$ depend on the *whole* history/memory of the material and its points. In our article we are especially concerned with the model of JIANG and SEHITOGLU, as it is quite successful in practice and widely accepted in the engineering community. It is rate-independent and reproduces many multiaxial stress-strain phenomena like nonlinear isotropic/kinematic hardening or ratchetting, see [14, 15]. We briefly name it *Jiang's model*. For an explicit representation of C^{ep} , we refer to (28).

Let us assume, we know the 'elastic' stress tensor ${}^e\sigma(t, x)$ via superposition of finitely many linear elastic, static PDE results, i.e.

$${}^e\sigma(t, x) = \sum_n L_n(t) {}^e\sigma_n(x), \quad {}^e\sigma_n(x) = C {}^e\varepsilon_n(x) \quad (2)$$

with given scalar load functions $L_n : [0, T] \rightarrow \mathbb{R}$. $C \in \mathbb{R}^{3 \times 3 \times 3 \times 3}$ is Hooke's tensor of elasticity

$$c_{ijkl} = \frac{E\nu}{(1+\nu)(1-2\nu)} \delta_{ij}\delta_{kl} + \frac{E}{1+\nu} \delta_{ik}\delta_{jl} = \lambda \delta_{ij}\delta_{kl} + 2\mu \delta_{ik}\delta_{jl} \quad (3)$$

($E =$ Young’s modulus, $\nu =$ Poisson’s ratio, $\lambda, \mu =$ Lamé’s constants). Due to the decoupling of time t and space x in (2) and due to the linear stress-strain relationship, the latter approach is numerically very cheap compared to the costs when solving the full transient problem with the exact nonlinear stress-strain relationship (1) with hysteresis.

- The **general case** (see \mathcal{K} in (10)): For $x \in \bar{U}$, we have ${}^e\sigma_n(x)$ and thus ${}^e\sigma(t, x)$ in

$$\mathbb{R}_s^{3 \times 3} = \{A \in \mathbb{R}^{3 \times 3} : A = A^T\} \simeq \mathbb{R}^6. \quad (4)$$

- The special **‘notch’ case** (see \mathcal{L} in (11)): If $x \in \partial U$, we know from the theory of linear elasticity, that an appropriate orthonormal basis exists such that all ${}^e\sigma_n(x)$ and thus ${}^e\sigma(t, x)$ are in

$$\mathbb{R}_{sp}^{3 \times 3} = \{A = (a_{ij}) \in \mathbb{R}_s^{3 \times 3} : a_{13} = a_{23} = a_{33} = 0\} \simeq \mathbb{R}_s^{2 \times 2} \simeq \mathbb{R}^3. \quad (5)$$

If x lies in an area, where the real stress is high, e.g. in a notched region, plasticity comes into play, so the elastic stress by far overestimates the real stress. Typically these regions are small, and the overall material behaviour is elastic.

Our goal is to rectify ${}^e\sigma(t) = {}^e\sigma(t, x)$ at *fixed* x in a postprocessing step to a better stress $\sigma(t) \in \mathbb{R}_s^{3 \times 3}$ resp. $\mathbb{R}_{sp}^{3 \times 3}$ – from now on referred to as the ‘real’ stress – by an appropriate modification of Jiang’s model, based on a pseudo parameter approach of KOETTGEN et al. [16].

Eventually, this is the point on which fatigue analysis may be set up. Instead of solving numerically expensive nonlinear PDE, we are focussing on a much cheaper nonlinear ODE model.

In this paper we will

1. give a proper definition of the correction model in [16], which is based on a strict coupling – we call it ‘simultaneity’ – between ‘elastic’ and ‘real’ stress space.
2. prove local existence and uniqueness for our correction model. Almost by the way, we will get local existence and uniqueness for Jiang’s constitutive model as well.
3. present an algorithm, which is more stable and faster than existing ones (e.g. [12, 16]) because of
 - (a) the strict simultaneity coupling in both stress spaces, which makes it possible to avoid iterative solution algorithms.
 - (b) a discontinuity detection for piecewise linear elastic stress inputs.

Remark 1.1 (fields of application) In engineering HCF-durability, e.g. in the automotive industry, load functions L_n are typically sampled with a frequency of approx. 400 sec^{-1} . One half hour on a test track would consequently yield about $7.2 \cdot 10^5$ data points. So it is – and will be in the next years – impossible to solve the full transient nonlinear PDE problem in an acceptable computational time with sufficiently fine finite element discretisation of the domain \bar{U} . Nowadays, a widespread practice to find a remedy is to correct scalar ‘equivalent’ signed norms/projections of ${}^e\sigma(t)$ via the ESED or NEUBER’s method, see e.g. [19].

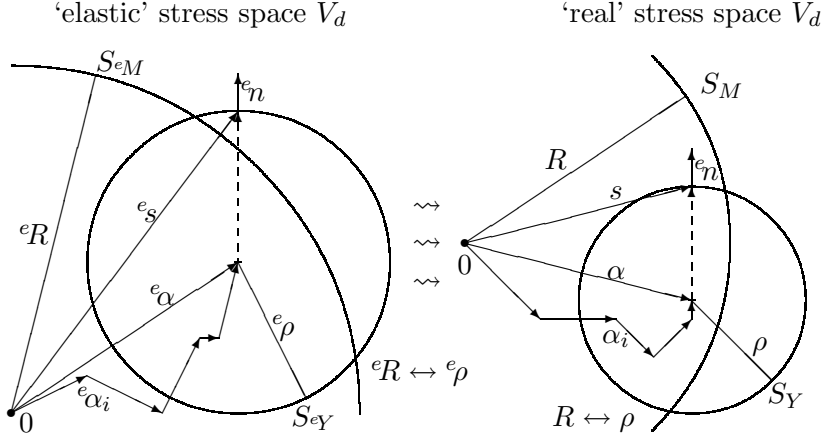


Figure 1: Movements in both stress spaces

1.2 Definition of the correction model

First, using the well known orthogonal decomposition

$$\mathbb{R}^{3 \times 3} = \mathbb{R}_d^{3 \times 3} \oplus \mathbb{R}_h^{3 \times 3} = \{A \in \mathbb{R}^{3 \times 3} : \text{tr } A = 0\} \oplus \mathbb{R}I \simeq \mathbb{R}^8 \oplus \mathbb{R}^1, \quad \mathbb{R}_d^{3 \times 3} \perp \mathbb{R}_h^{3 \times 3}$$

with the associated linear orthogonal projections $\text{dev} : \mathbb{R}^{3 \times 3} \rightarrow \mathbb{R}_d^{3 \times 3}$ and $\text{sph} : \mathbb{R}^{3 \times 3} \rightarrow \mathbb{R}_h^{3 \times 3}$ we define

$$\mathbb{R}_{sd}^{3 \times 3} = \text{dev } \mathbb{R}_s^{3 \times 3} = \{A \in \mathbb{R}_s^{3 \times 3} : a_{33} = -a_{11} - a_{22}\} \simeq \mathbb{R}^5, \quad (6)$$

$$\mathbb{R}_{spd}^{3 \times 3} = \text{dev } \mathbb{R}_{sp}^{3 \times 3} = \{A \in \mathbb{R}_s^{3 \times 3} : a_{13} = a_{23} = 0, a_{33} = -a_{11} - a_{22}\} \simeq \mathbb{R}^3, \quad (7)$$

which are deviatoric subspaces of $\mathbb{R}_s^{3 \times 3}$, corresponding to (4) and (5). Our indices s, p, d and h mean symmetric, plane, deviatoric and hydrostatic (i.e. spherical).

Notation. Let \cdot and $\|\cdot\|$ denote the standard Euklidian scalar product resp. norm on $\mathbb{R}^{3 \times 3} \simeq \mathbb{R}^9$, $B_r(\sigma) = \{\tau \in \mathbb{R}_s^{3 \times 3} : \|\tau - \sigma\| < r\}$ and

$$\pi : \mathbb{R}_s^{3 \times 3} \rightarrow \partial B_1(0), \quad \sigma \mapsto \begin{cases} \sigma / \|\sigma\| & \text{if } \sigma \neq 0 \\ 0 & \text{if } \sigma = 0 \end{cases}.$$

The underlying function spaces are

$$\begin{aligned} \mathcal{C}^k([0, T], \cdot) &= \text{space of } k\text{-times continuously differentiable functions,} \\ \mathcal{C}_{pw}^k([0, T], \cdot) &= \text{space of piecewise } \mathcal{C}^k \text{ functions,} \\ \mathcal{AC}([0, T], \cdot) &= \text{space of absolutely continuous functions} \end{aligned}$$

where the respective image depends on the context. Note that $\mathcal{AC} = \mathcal{W}^{1,1}$.

A. We assume that symmetric elastic stresses ${}^e\sigma \in \mathcal{C}_{pw}^1([0, T], V)$, where V is either $\mathbb{R}_s^{3 \times 3}$ or $\mathbb{R}_{sp}^{3 \times 3}$, are given. Their deviatoric parts

$${}^e\dot{s}(t) = \text{dev}({}^e\dot{\sigma}(t)), \quad {}^e\dot{s}(t) = \text{d}_t {}^e s(t) = \text{dev}({}^e\dot{\sigma}(t)) \quad (8)$$

are external input/force into

$$(\dot{\varepsilon}^{pl}, \dot{\xi}, \dot{\alpha}_1, \dots, \dot{\alpha}_m, \dot{R}, \dot{\alpha}_1, \dots, \dot{\alpha}_m, \dot{R}) = \mathcal{J}_{e_s}(t, \xi, \alpha_1, \dots, \alpha_m, R, \alpha_1, \dots, \alpha_m, R) \quad (9)$$

a system of first order discontinuous ordinary differential equations. That way, \mathcal{J}_{e_s} is explicitly time dependent, the so called *elastic stress control*.

B. After solving ODE (9), the real stress deviators $s(t)$ are defined *simultaneously* (i.e. *parallel* and *rescaled*) to the elastic stress deviators ${}^e s(t)$ at the corresponding point in real stress space

$$(\sigma, \varepsilon, \varepsilon^{el}, s, \alpha, \rho, \alpha, \rho) = \mathcal{K}({}^e s, \varepsilon^{pl}, \alpha_1, \dots, \alpha_m, R, \alpha_1, \dots, \alpha_m, R, \sigma_h) \quad (10)$$

$$\text{resp. } (\sigma, \varepsilon, \varepsilon^{el}, s, \alpha, \rho, \alpha, \rho) = \mathcal{L}({}^e s, \varepsilon^{pl}, \alpha_1, \dots, \alpha_m, R, \alpha_1, \dots, \alpha_m, R), \quad (11)$$

each a system of simple explicit algebraic equations.

For a better geometric understanding, we refer to figure 1. There are a lot of parameters appearing in the definition of \mathcal{J}_{e_s} , \mathcal{L} , \mathcal{K} , which are all listed in (20) below.

A. Definition of \mathcal{J}_{e_s} on

$$\Omega = [0, T] \times \mathbb{R} \times V_d^m \times (0, \infty) \times V_d^m \times (0, \infty)$$

where

$$V_d = \text{dev } V \text{ from (6), i.e. } V = \mathbb{R}_s^{3 \times 3}, \text{ or (7), i.e. } V = \mathbb{R}_{sp}^{3 \times 3}.$$

For $(t, \xi, \alpha_1, \dots, \alpha_m, R, \alpha_1, \dots, \alpha_m, R) \in \Omega$ we set

$${}^e \rho = {}^e \rho_0 (1 + {}^e a_\rho e^{{}^e b_\rho R}), \quad {}^e \alpha = \sum_{j=1}^m {}^e \alpha_j, \quad \alpha = \sum_{j=1}^m \alpha_j. \quad (12)$$

and

$$S_{eY} = \partial B_{e\rho}({}^e \alpha) \quad \text{the 'elastic' yield surface,} \quad (13a)$$

$$S_{eM} = \partial B_{eR}(0) \quad \text{the 'elastic' memory surface,} \quad (13b)$$

$$S_M = \partial B_R(0) \quad \text{the 'real' memory surface.} \quad (13c)$$

Now if ${}^e s(t) \in B_{e\rho}({}^e \alpha)$ (*no loading*, i.e. elastic), define for $i = 1, \dots, m$

$$\dot{\varepsilon}^{pl} = 0, \quad \dot{\xi} = 0, \quad \dot{\alpha}_i = 0, \quad \dot{R} = 0, \quad \dot{\alpha}_i = 0, \quad \dot{R} = 0. \quad (14)$$

Otherwise we declare

$${}^e n = {}^e n(t, \alpha_1, \dots, \alpha_m) = \pi({}^e s(t) - {}^e \alpha), \quad {}^e \dot{s}_n = {}^e \dot{s}(t) : {}^e n.$$

If ${}^e \dot{s}_n \leq 0$ (*neutral loading*), let (14) hold again, else (*plastic loading*) set for $i = 1, \dots, m$

$${}^e \chi_i = {}^e Q_i (2 - {}^e n : \pi({}^e \alpha_i)) (1 + {}^e a_\chi e^{{}^e b_\chi R}) \quad (15a)$$

$${}^e c_i = {}^e c_i^\infty \left(1 + {}^e a_i^{(1)} e^{-{}^e b_i^{(1)} \xi} + {}^e a_i^{(2)} e^{-{}^e b_i^{(2)} \xi} \right) \quad (15b)$$

$$d_\xi {}^e \alpha_i = {}^e c_i {}^e r_i \left({}^e n - \left(\frac{\|{}^e \alpha_i\|}{{}^e r_i} \right)^{{}^e \chi_i + 1} \pi({}^e \alpha_i) \right) \quad (15c)$$

$$d_\xi {}^e \alpha = \sum_{j=1}^m d_\xi {}^e \alpha_j \quad (15d)$$

$$d_\xi {}^e R = \begin{cases} -{}^e c_R (1 - \|{}^e \alpha\| / {}^e R) & \text{if } {}^e \alpha \in B_{eR}(0) \\ (\pi({}^e \alpha) : d_\xi {}^e \alpha)^+ & \text{if } {}^e \alpha \in B_{eR}(0)^c \end{cases} \quad (15e)$$

in the ‘elastic stress space’, and

$$\chi_i = Q_i(2 - {}^e n : \pi(\alpha_i))(1 + a_\chi e^{b_\chi R}) \quad (16a)$$

$$c_i = c_i^\infty \left(1 + a_i^{(1)} e^{-b_i^{(1)} \xi} + a_i^{(2)} e^{-b_i^{(2)} \xi}\right) \quad (16b)$$

$$d_\xi \alpha_i = c_i r_i \left({}^e n - \left(\frac{\|\alpha_i\|}{r_i} \right)^{\chi_i+1} \pi(\alpha_i) \right) \quad (16c)$$

$$d_\xi \alpha = \sum_{j=1}^m d_\xi \alpha_j \quad (16d)$$

$$d_\xi R = \begin{cases} -c_R(1 - \|\alpha\|/R) & \text{if } \alpha \in B_R(0) \\ (\pi(\alpha) : d_\xi \alpha)^+ & \text{if } \alpha \in B_R(0)^c \end{cases} \quad (16e)$$

in the ‘real stress space’. Further, we declare

$$d_\xi {}^e \rho = {}^e \rho_0 {}^e a_\rho {}^e b_\rho e^{{}^e b_\rho {}^e R} d_\xi {}^e R, \quad {}^e h = {}^e n : d_\xi {}^e \alpha + d_\xi {}^e \rho. \quad (17)$$

The values of \mathcal{J}_{e_s} are finally given by

$${}^e \dot{R} = \dot{\xi} d_\xi {}^e R, \quad {}^e \dot{\alpha}_i = \dot{\xi} d_\xi {}^e \alpha_i, \quad \dot{\xi} = \frac{{}^e \dot{s}_n}{{}^e h}, \quad \varepsilon^{pl} = \dot{\xi} {}^e n, \quad \dot{R} = \dot{\xi} d_\xi R, \quad \dot{\alpha}_i = \dot{\xi} d_\xi \alpha_i. \quad (18)$$

Of course, ${}^e \alpha_i$, α_i , ε^{pl} remain in V , as V is a linear space. We remark that the right hand-side of (9) does not depend on ε^{pl} .

The initial values for (9). We assume that they satisfy the following conditions:

$$0 < \|{}^e \alpha_i(0)\| < {}^e r_i, \quad 0 < \left\| \sum_{j=1}^m {}^e \alpha_j(0) \right\| \leq {}^e R(0), \quad (19a)$$

$$0 < \|\alpha_i(0)\| < r_i, \quad 0 < \left\| \sum_{j=1}^m \alpha_j(0) \right\| \leq R(0), \quad (19b)$$

$$\varepsilon^{pl}(0) \text{ arbitrary, } \xi(0) \geq 0, \quad (19c)$$

$$\left\| {}^e s(0) - \sum_{j=1}^m {}^e \alpha_j(0) \right\| \leq {}^e \rho_0 (1 + {}^e a_\rho e^{{}^e b_\rho {}^e R(0)}). \quad (19d)$$

For virgin material we should additionally have ${}^e \alpha_i(0) = \alpha_i(0)$, ${}^e R(0) = R(0)$ and $\|{}^e \alpha_i(0)\| \ll 1$, ${}^e R(0) \ll 1$ and ${}^e \sigma(0) = 0$.

The parameters for (9). We need ‘elastic parameters’ ${}^e p_l$ for the elastic stress space, and ‘real parameters’ p_l for the real stress space, namely

$${}^e a_i^{(j)}, {}^e a_\chi \in \mathbb{R}; \quad {}^e b_\chi \leq 0 \leq {}^e Q_i; \quad -1 < {}^e a_\rho < 0; \quad {}^e b_\rho < 0 < {}^e b_i^{(j)}, {}^e c_R, {}^e r_i, {}^e c_i^\infty, {}^e \rho_0 \quad (20a)$$

$$a_i^{(j)}, a_\chi \in \mathbb{R}; \quad b_\chi \leq 0 \leq Q_i; \quad -1 < a_\rho < 0; \quad b_\rho < 0 < b_i^{(j)}, c_R, r_i, c_i^\infty, \rho_0 \quad (20b)$$

$l = 1, \dots, 7m + 6$, $i = 1, \dots, m$, $j = 1, 2$. The ${}^e a_i^{(j)}$, ${}^e b_i^{(j)}$, $a_i^{(j)}$, $b_i^{(j)}$ have to be chosen in such a way that

$$\inf_{\xi \geq 0} \sum_j {}^e a_i^{(j)} e^{-{}^e b_i^{(j)} \xi} > -1, \quad \inf_{\xi \geq 0} \sum_j a_i^{(j)} e^{-b_i^{(j)} \xi} > -1 \quad (i = 1, \dots, m) \quad (21)$$

The p_l are physical parameters (‘Jiang parameters’), depending solely on the material, whereas the ${}^e p_l$ are fictive and depend additionally on the considered point x , in particular on the

geometry of U . For each x we need an appropriate set of ${}^e p_l$. The affects of p_l resp. ${}^e p_l$ on the material/part properties as ratchetting or cyclic hardening/softening are explained in [14, 15]. In any case, we should have ${}^e \rho_0(1 + {}^e a_\rho) \approx \rho_0(1 + a_\rho)$, as $R \approx {}^e R$ for virgin material, see (29) and [12], chap. 4.

B. Definition of \mathcal{L} (the special ‘notch case’, $V = \mathbb{R}_{sp}^{3 \times 3}$) on

$$V^{[0,T]} \times V_d^{[0,T]} \times \left(V_d^{[0,T]}\right)^m \times (0, \infty)^{[0,T]} \times \left(V_d^{[0,T]}\right)^m \times (0, \infty)^{[0,T]}.$$

For all $0 \leq t \leq T$ we set ${}^e \rho(t)$, ${}^e \alpha(t)$, $\alpha(t)$ as in (12) and

$$\rho(t) = \rho_0(1 + a_\rho e^{b_\rho R(t)}), \quad s(t) = \alpha(t) + \frac{\rho(t)}{{}^e \rho(t)} ({}^e s(t) - {}^e \alpha(t)). \quad (22)$$

The ‘real’ yield surface is defined as $S_Y(t) = \partial B_{\rho(t)}(\alpha(t))$. Finally the real stress and strains are

$$\sigma(t) = D^{-1}s(t), \quad \varepsilon^{el}(t) = C^{-1}\sigma(t), \quad \varepsilon(t) = \varepsilon^{el}(t) + \varepsilon^{pl}(t). \quad (23)$$

where D is the linear isomorphism

$$D = \mathbb{R}_{spd}^{3 \times 3} | \text{dev} |_{\mathbb{R}_{sp}^{3 \times 3}} : \mathbb{R}_{sp}^{3 \times 3} \rightarrow \mathbb{R}_{spd}^{3 \times 3}.$$

If ${}^e \sigma$ and σ are not plane, our correction is applicable too, but only if the hydrostatic component σ_h is available as additional information.

Definition of \mathcal{K} (the general case, $V = \mathbb{R}_s^{3 \times 3}$) on

$$V^{[0,T]} \times V_d^{[0,T]} \times \left(V_d^{[0,T]}\right)^m \times (0, \infty)^{[0,T]} \times \left(V_d^{[0,T]}\right)^m \times (0, \infty)^{[0,T]} \times \mathbb{R}^{[0,T]}.$$

Here the same equations as for \mathcal{L} hold, except that we replace the first equation in (23) by $\sigma(t) = s(t) + \sigma_h(t)I$.

The parameters for (10) and (11). Here we just have $E > 0$ and $0 < \nu < 1/2$ in (3). But note that they don’t have any affect on σ .

Remark 1.2 (simultaneity) By definition (22) we enforce parallelity of ${}^e s - {}^e \alpha$ and $s - \alpha$. Note that in (15d) and (16d) the same yield surface normal ${}^e n$ is used both for ${}^e S_Y$ and S_Y . That’s the way, the movements in both stress spaces are coupled. The movement of the ${}^e \alpha_i$ and α_i (and thus ${}^e \alpha$ and α) and the development of ${}^e R$ and R differ in general, unless ${}^e p_l$ are p_l equal. For illustration see again figure 1, where $m = 5$.

Remark 1.3 (former work) Defining \mathcal{J}_{e_s} , \mathcal{L} and \mathcal{K} , we clearly follow the idea of KOETTGEN et al. [16], which they call the ‘ ${}^e \sigma$ –approach’. They developed this kind of scheme for the constitutive model of MROZ [18]. Later HERTEL [12] adapted this approach to Jiang’s model. But compared to our formulation, there are some differences in [12, 16]:

- The integration of

$$\dot{s} = \frac{h}{e^h} e^s, \quad h = e^n : d_\xi \alpha + d_\xi \rho \quad (24)$$

proposed in [16] cannot be realized in a consistent manner with the fact that Jiang's model comprises expansion/contraction of the yield surface. So, during integration of (24), we have two yield surfaces with different radii ρ and $e\rho$ and thus two yield conditions to be satisfied at the same time, which is inconsistent with the simultaneity idea. In contrast to our case, a purely kinematic version of Mroz's model with only one yield condition ($e\rho = \rho$) is referred to in [16].

An additional advantage of our formulation is that we get rid of equation (24), so the number of differential equations to be integrated is reduced.

- As the physical correction idea is per definition simultaneous, we are integrating the equations in elastic and real stress space parallelly coupled and *not* iteratively in series

$$e\sigma(t) \xrightarrow{(25), e^{\rho_i}} \varepsilon^{pl}(t) \xrightarrow{\text{Iter.}, \rho_i} \sigma(t),$$

as it is done in [12, 16]. So, as we don't have a stress-controlled integration followed by completely separated strain-controlled integrations, this yields more accuracy and much more speed, as we have to handle the problems with discontinuities only once. We have the guarantee that plastic yielding starts/stops exactly at the same point in time. That way, our algorithm has turned out to decrease the number of expensive function evaluation by a factor more than 21 compared to [12] yielding a speed factor of more than 10.

Remark 1.4 (the original stress controlled Jiang model) Since $e\dot{\alpha}_i$, $e\dot{R}$, $\dot{\xi}$, $\dot{\varepsilon}^{pl}$ do not depend on α_i , R_i , you rediscover the original stress-controlled Jiang model [14] as a subsystem

$$(\dot{\varepsilon}^{pl}, \dot{\xi}, \dot{\alpha}_1, \dots, \dot{\alpha}_m, \dot{R}) = \mathcal{J}_s(t, \xi, \alpha_1, \dots, \alpha_m, R) \quad (25)$$

on

$$\Omega = [0, T] \times \mathbb{R} \times V_d^m \times (0, \infty),$$

where $s = \text{dev}(\sigma) \in C_{pw}^1([0, T], V_d)$ is the external input and $\varepsilon = C^{-1}\sigma + \varepsilon^{pl}$. Just drop the additional equations (16) and the e at each 'elastic' variable and parameter. Here the elastic stress and the real stress space coincide, under the assumption that the input (8) is the real stress, (13c) does not exist. The initial values/conditions analogous to (19) are

$$0 < \|\alpha_i(0)\| < r_i, \quad 0 < \left\| \sum_{j=1}^m \alpha_j(0) \right\| \leq R(0) \quad (26a)$$

$$\varepsilon^{pl}(0) \text{ arbitrary}, \quad \xi(0) \geq 0 \quad (26b)$$

$$\left\| s(0) - \sum_{j=1}^m \alpha_j(0) \right\| \leq \rho_0(1 + a_\rho e^{b_\rho R(0)}). \quad (26c)$$

Condition (30) becomes ($\epsilon > 0$ small)

$$\sum_{j=1}^m c_j(r_j - \|\alpha_j\|) \geq \rho_0 a_\rho b_\rho c_R + \epsilon. \quad (27)$$

It can be straight forwardly shown that in (1)

$$C^{ep} = C \left(I - \frac{2\mu}{2\mu + h} n \otimes n \right). \quad (28)$$

2 Local existence and uniqueness of solution

The ('elastic') stress controlled functions \mathcal{J}_{e_s} in (9) and \mathcal{J}_s in (25) are discontinuous. So unfortunately, the standard theory of systems of ordinary differential equations, where usually at least local Lipschitz continuity is required, does not apply. We need a generalized solution concept to guarantee one and only one solution of the respective systems of equations.

For other elastoplastic constitutive laws comprising nonlinear kinematic hardening – e.g. the models of Melan-Prager, Armstrong-Frederick or Chaboche – wellposedness results are already available. The reader is referred to the work of BROKATE/KREJCI [2, 3, 4]. The mathematical techniques there rely on the theory of variational evolution inequalities and moving convex sets in Hilbert spaces.

However, this is not easily applicable here, as Jiang's model additionally comprises nonlinear isotropic hardening, i.e. the yield surface – the convex set in Brokate's theory – may contract and expand. So in this paper, we will study a completely different approach. We will consider (9) resp. (25) as differential inclusions in order to apply the theory of FILIPPOV [9].

2.1 First analytical facts

Lemma 2.1 *The yield and memory radii are coupled in a one-to-one manner. The mappings*

$$(0, \infty) \ni {}^e R \xrightarrow{ef} {}^e \rho \in (0, \infty) \text{ in (12)}, \quad (0, \infty) \ni R \xrightarrow{f} \rho \in (0, \infty) \text{ in (22)}$$

are strictly increasing. Further

$${}^e \rho \xrightarrow{{}^e R \rightarrow \infty} {}^e \rho_0, \quad \rho \xrightarrow{R \rightarrow \infty} \rho_0, \quad (29a)$$

$${}^e \rho \xrightarrow{{}^e R \rightarrow 0} {}^e \rho_0(1 + {}^e a_\rho) = {}^e \sigma_Y, \quad \rho \xrightarrow{R \rightarrow 0} \rho_0(1 + a_\rho) = \sigma_Y. \quad (29b)$$

Especially

$$0 < {}^e \sigma_Y \leq {}^e \rho \leq {}^e \rho_0 < \infty, \quad 0 < \sigma_Y \leq \rho \leq \rho_0 < \infty.$$

The inverse mappings are given by

$${}^e \rho \xrightarrow{{}^e f^{-1}} \frac{1}{{}^e b_\rho} \ln \left(\frac{{}^e \rho / {}^e \rho_0 - 1}{{}^e a_\rho} \right), \quad \rho \xrightarrow{f^{-1}} \frac{1}{b_\rho} \ln \left(\frac{\rho / \rho_0 - 1}{a_\rho} \right).$$

Proof: Clear, because $a_\rho, b_\rho, {}^e a_\rho, {}^e b_\rho < 0 < \rho_0, {}^e \rho_0$. ■

So it doesn't matter which of ${}^e R$ or ${}^e \rho$ to choose as the governing variable. We decided to take ${}^e R$.

Lemma 2.2 *If $\|{}^e \alpha_i\| \leq {}^e r_i$, then $d_\xi {}^e \alpha_i : {}^e n \geq 0$. If $\|{}^e \alpha_i\| \leq {}^e r_i$ for all $i = 1, \dots, m$ and at least one of the inequalities is strict, then $d_\xi {}^e \alpha : {}^e n > 0$. The analogous assertions hold for $d_\xi \alpha$ and ${}^e n$.*

Proof: For each i , multiplication of (15c) with ${}^e n$ yields using the Cauchy-Schwarz inequality

$$d_\xi {}^e \alpha_i : {}^e n = {}^e c_i {}^e r_i \left(1 - \left(\frac{\|{}^e \alpha_i\|}{{}^e r_i} \right)^{\chi_i + 1} {}^e n : \pi({}^e \alpha_i) \right) \geq 0$$

(note that ${}^e\chi \geq 0$) with at least one strict inequality, and therefore the assertions follow after summing over $i = 1, \dots, m$. \blacksquare

During elastic/neutral loading, $\dot{\xi} = \|\dot{\varepsilon}^{pl}\| = 0$ due to (14). During plastic loading, we conclude from (18) – the next lemma will guarantee ${}^e h > {}^e h_{\min} > 0$ – that $0 < \dot{\xi} = \|\dot{\varepsilon}^{pl}\| \leq \dot{\xi}_{\max}$. Therefore $\xi(t) = \int_0^t \|\dot{\varepsilon}^{pl}(\tau)\| d\tau$ is the accumulated plastic strain: constant during elastic/neutral loading and strictly increasing during plastic loading, in particular non-negative due to the initial condition (19c).

Lemma 2.3 *If $\|\alpha_i\| \leq r_i$ for $i = 1, \dots, m$, a sufficient condition for ${}^e h \geq {}^e h_{\min} > 0$ (or equivalently $0 < \dot{\xi} \leq \dot{\xi}_{\max}$) is*

$$\sum_{j=1}^m {}^e c_j ({}^e r_j - \|\alpha_i\|) \geq {}^e \rho_0 {}^e a_\rho {}^e b_\rho {}^e c_R + \epsilon \quad (30)$$

with an $\epsilon > 0$.

Proof: In both cases in (15e), we have

$$d_\xi {}^e R \geq -{}^e c_R (1 - \|\alpha\|/{}^e R) \geq -{}^e c_R \quad (31)$$

Hence

$$\begin{aligned} {}^e h &\stackrel{(15c, 15d, 17)}{=} \sum_j {}^e c_j {}^e r_j \left(1 - \left(\frac{\|\alpha_j\|}{{}^e r_j} \right)^{\chi_j+1} {}^e n : \pi(\alpha_j) \right) + {}^e \rho_0 {}^e a_\rho {}^e b_\rho e^{\chi_j} d_\xi {}^e R \\ &\stackrel{(31)}{\geq} \sum_j {}^e c_j {}^e r_j (1 - \|\alpha_i\|/{}^e r_i) - {}^e \rho_0 {}^e a_\rho {}^e b_\rho {}^e c_R \end{aligned}$$

Note here that ${}^e \chi_i \geq 0 > {}^e a_\rho, {}^e b_\rho$. As ${}^e s$ is bounded over any interval $[t_{n-1}, t_n]$, where ${}^e s \in \mathcal{C}^1$, ${}^e \dot{s} \in \mathcal{C}^0$, it is in fact globally bounded on $[0, T]$, thus $\dot{\xi} \leq \dot{\xi}_{\max} < \infty$. \blacksquare

The next lemma proves that the α_i ‘remain in their limiting radii’ r_i as already asserted (but *not* proved) in [15] in the case of proportional monotonous loading.

Lemma 2.4 *Let ${}^e n \in \mathcal{C}_{pw}^1([\xi_0, \xi_T], V_d \cap \partial B_1(0))$, where $0 \leq \xi_0 < \xi_T < \infty$, be given as input into the differential equations for the partial backstresses (15a)-(15c) and (16a)-(16c). Then each $\alpha_i \in \mathcal{C}_{pw}^1([\xi_0, \xi_T], V_d)$. If $\|\alpha_i(\xi_0)\| < r_i$, then $\|\alpha_i(\xi)\| < r_i$ holds in the whole interval $[\xi_0, \xi_T]$. The analogous assertion holds for α_i and r_i instead of α_i and r_i .*

Proof: Obviously, since all $\mathfrak{b}_i^{(j)} > 0$ and $\xi \geq \xi_0 \geq 0$, we have

$$0 < 1 + {}^e I < {}^e c_i \stackrel{(15b)}{\leq} {}^e c_i^\infty \left(1 + |{}^e a_i^{(1)}| + |{}^e a_i^{(2)}| \right) =: {}^e C_i. \quad (32)$$

where ${}^e I$ denotes the infimum in (21). Let us first consider the interval $[\xi_0, \xi_1]$, where ${}^e n$ is \mathcal{C}^1 . Here we have the polar decomposition $\alpha_i = \|\alpha_i\| \pi(\alpha_i)$. Differentiation with respect to ξ yields

$$d_\xi \|\alpha_i\| \pi(\alpha_i) + \|\alpha_i\| d_\xi \pi(\alpha_i) = d_\xi \alpha_i \stackrel{(15c)}{=} {}^e c_i {}^e r_i \left({}^e n - \left(\frac{\|\alpha_i\|}{r_i} \right)^{\chi_i+1} \pi(\alpha_i) \right). \quad (33)$$

Since $1 = \|\pi({}^e\alpha_i)\|^2$, we have $0 = d_\xi \|\pi({}^e\alpha_i)\|^2 = 2\pi({}^e\alpha_i) : d_\xi \pi({}^e\alpha_i)$, and therefore after scalar multiplication of (33) with $\pi({}^e\alpha_i)$

$$d_\xi \|{}^e\alpha_i\| = {}^e c_i {}^e r_i \left({}^e n : \pi({}^e\alpha_i) - \left(\frac{\|{}^e\alpha_i\|}{{}^e r_i} \right)^{{}^e\chi_i+1} \right) \stackrel{(32)}{\leq} {}^e C_i {}^e r_i \left(1 - \left(\frac{\|{}^e\alpha_i\|}{{}^e r_i} \right)^{{}^e\chi_i+1} \right).$$

As ${}^e b_\chi \leq 0$, we have ${}^e\chi_i+1 \leq 1+3{}^e Q_i(1+|{}^e a_\chi|) =: {}^e K_i$, and with the substitution ${}^e\gamma_i = \|{}^e\alpha_i\|/{}^e r_i$ we obtain the scalar radial differential inequality

$$d_\xi {}^e\gamma_i \leq {}^e C_i \left(1 - {}^e\gamma_i^{{}^e K_i} \right).$$

In both cases ${}^e K_i > 1$ and ${}^e K_i = 1$, separating the variables leads us to ${}^e\gamma_i < 1$. \blacksquare

$\|{}^e\alpha_i\|$ (in the worst case *each*) may asymptotically reach ${}^e r_i$ and the first summand in (30) may become too small and the whole model bursts. This usually occurs, if the inputs ${}^e s(t)$ are too large. Anyway the model (9) is just able to get along with inputs that are small enough. So far, we have not been able to prove a sufficient a-priori-estimate depending on the $\mathcal{W}^{1,1}$ norm $\|{}^e s\|_{1,1}$ of the input like – for example – Brokate did in [2, 3] for elastoplasticity models of lower complexity. A way to find a remedy in practice is to use *more* backstresses. Unfortunately, a larger m yields more differential equations and more parameters.

2.2 Proof of the main theorem

Let us first consider the Jiang correction model. For our theoretical purposes, we rewrite (9) equivalently in the form

$$\dot{y} = \mathcal{J}_{e_s}(t, y), \quad y = (\varepsilon^{pl}, \xi, {}^e\alpha_1, \dots, {}^e\alpha_m, {}^e R, \alpha_1, \dots, \alpha_m, R)$$

or

$$\dot{x} = \mathcal{I}_{e_s}(x) = (1, \mathcal{J}_{e_s}(x)), \quad x = (t, y). \quad (34)$$

Through introduction of time as an artificial space variable $x_0 = t$, the system (34) is autonomous and we have pushed our time discontinuity into space. We prove existence and uniqueness of a Filippov-solution $t \mapsto x(t)$ of the differential inclusion

$$\dot{x} \in \mathfrak{J}_{e_s}(x) = \text{conv} \left\{ v : \exists (x_k)_{k \in \mathbb{N}} \subset \Omega \text{ s.t. } x_k \xrightarrow{k \rightarrow \infty} x \text{ and } \mathcal{I}_{e_s}(x_k) \xrightarrow{k \rightarrow \infty} v \right\},$$

i.e. a function $x \in \mathcal{AC}([0, T], \Omega)$,

$$\Omega = [0, T] \times V_d \times \mathbb{R} \times V_d^m \times (0, \infty) \times V_d^m \times (0, \infty)$$

satisfying (34) for almost every t . Of course, if \mathcal{I}_{e_s} is continuous in x , we have $\mathfrak{J}_{e_s}(x) = \{\mathcal{I}_{e_s}(x)\}$. The set of discontinuity points of \mathcal{I}_{e_s} has measure zero. More precisely speaking, it is given by $S_{e_Y}^\Omega \cup S_{e_M}^\Omega \cup S_M^\Omega$ with the smooth submanifolds (cylinders)

$$S_{e_Y}^\Omega = \{x \in \Omega : \varphi_{e_Y}(x) = 0\}, \quad \varphi_{e_Y}(x) = \left\| {}^e s(t) - \sum_j {}^e \alpha_j \right\| - {}^e \rho_0 (1 + {}^e a_\rho e^{{}^e b_\rho} {}^e R), \quad (35a)$$

$$S_{e_M}^\Omega = \{x \in \Omega : \varphi_{e_M}(x) = 0\}, \quad \varphi_{e_M}(x) = \left\| \sum_j {}^e \alpha_j \right\| - {}^e R, \quad (35b)$$

$$S_M^\Omega = \{x \in \Omega : \varphi_M(x) = 0\}, \quad \varphi_M(x) = \left\| \sum_j \alpha_j \right\| - R, \quad (35c)$$

separating Ω into the domains

$$\Omega_{e_Y}^- = \{x : \varphi_{e_Y} < 0\}, \quad \Omega_{e_M}^- = \{x : \varphi_{e_M} < 0\}, \quad \Omega_M^- = \{x : \varphi_M < 0\}, \quad (36a)$$

$$\Omega_{e_Y}^+ = \{x : \varphi_{e_Y} > 0\}, \quad \Omega_{e_M}^+ = \{x : \varphi_{e_M} > 0\}, \quad \Omega_M^+ = \{x : \varphi_M > 0\}, \quad (36b)$$

where \mathcal{I}_{e_s} is Lipschitz and the solution x therefore will be smooth.

Remark 2.5 (γ -condition) All of the domains (36) and all their mutual intersections

$$\Omega_{e_Y e_M}^{-+} = \Omega_{e_Y}^- \cap \Omega_{e_M}^+, \dots, \quad \Omega_{e_Y e_M M}^{-++} = \Omega_{e_Y}^- \cap \Omega_{e_M}^+ \cap \Omega_M^+, \dots$$

are locally connected, as a consequence they satisfy Filippov's γ -condition, i.e.

$$(\partial\Omega_{e_Y}^-) \cap \{t = \text{const}\} = \partial(\Omega_{e_Y}^- \cap \{t = \text{const}\}) \quad \text{for almost all } t, \dots$$

(see [9], §6) where the boundary ∂ at the right hand side is to be taken in the relative topology of the hyperplane $\{t = \text{const}\}$. The whole theory ([9], §7, §9, §10) is developed for discontinuities in the space variable x . But in [9], §6 and §9, it is shown that under the γ -condition the introduction of dummy time x_0 above does not influence solution properties, i.e. existence and uniqueness.

In the sequel, we assume that ${}^e s_n = {}^e n \cdot {}^e s > 0$, where the discontinuities at the surfaces $S_{e_Y}^\Omega$, $S_{e_M}^\Omega$ and S_M^Ω occur. In the case ${}^e s_n \leq 0$, due to (14), the whole movements, i.e. the functions ε^{pl} , ξ , ${}^e \alpha_i$, ${}^e R$, α_i and R , remain constant.

1. We first consider the active loading of $S_{e_Y}^\Omega$, i.e. the the case, where the solution reaches a point $x \in S \cap \Omega_{e_M}^-$, $S = S_{e_Y}^\Omega = \partial\Omega_{e_Y}^- = \partial\Omega_{e_Y}^+$. Here we have $\mathcal{J}_{e_s} = \text{conv}\{\mathcal{I}^-, \mathcal{I}^+\}$ with functions

$$\begin{aligned} \mathcal{I}^-(x) &= \lim_{x' \in \Omega_{e_Y}^-, x' \rightarrow x} \mathcal{I}_{e_s}(x') = (1, \mathbf{0}, 0, \mathbf{0}, \dots, \mathbf{0}, 0, \mathbf{0}, \dots, \mathbf{0}, 0) \\ \mathcal{I}^+(x) &= \lim_{x' \in \Omega_{e_Y}^+, x' \rightarrow x} \mathcal{I}_{e_s}(x') \\ &= \left(1, \star, \star, {}^e c_1 \left({}^e n - \left(\frac{\|{}^e \alpha_1\|}{{}^e r_1} \right)^{{}^e \chi_1} {}^e \alpha_1 \right) \dot{\xi}, \dots, {}^e c_m \left({}^e n - \left(\frac{\|{}^e \alpha_m\|}{{}^e r_m} \right)^{{}^e \chi_m} {}^e \alpha_m \right) \dot{\xi}, \right. \\ &\quad \left. - {}^e c_R \left(1 - \frac{\|{}^e \alpha\|}{{}^e R} \right) \dot{\xi}, \star, \dots, \star, \star \right) \end{aligned}$$

which are smooth up to $\bar{\Omega}_{e_Y}^-$ and $\bar{\Omega}_{e_Y}^+$ respectively. \star and \star denote some scalar resp. tensorial quantities. To have a unique element $\mathcal{I}^0 = \lambda^- \mathcal{I}^- + \lambda^+ \mathcal{I}^+ \in \mathcal{J}_{e_s} \cap \mathcal{T}_x S$, it is necessary and sufficient that the system of linear equations

$$\begin{pmatrix} 1 & 1 \\ \langle \nabla \varphi_{e_Y}, \mathcal{I}^- \rangle & \langle \nabla \varphi_{e_Y}, \mathcal{I}^+ \rangle \end{pmatrix} \begin{pmatrix} \lambda^- \\ \lambda^+ \end{pmatrix} = \begin{pmatrix} 1 \\ 0 \end{pmatrix}$$

has one and only one solution. Vector calculus leads us to

$$\nabla \varphi_{e_Y} = ({}^e \dot{s}_n, \mathbf{0}, 0, -{}^e n, \dots, -{}^e n, -{}^e \rho_0 {}^e a_\rho {}^e b_\rho e^{{}^e b_\rho} {}^e R, \mathbf{0}, \dots, \mathbf{0}, 0)$$

The projections of the function value limits on the surface normal are $\langle \nabla \varphi_{e_Y}, \mathcal{I}^- \rangle = {}^e \dot{s}_n > 0$ and

$$\begin{aligned} & \langle \nabla \varphi_{e_Y}, \mathcal{I}^+ \rangle \\ &= {}^e \dot{s}_n - \sum_j {}^e c_j \left({}^e n - \left(\frac{\|{}^e \alpha_j\|}{e_{r_j}} \right)^{\chi_j} {}^e \alpha_j \right) \dot{\xi} + {}^e \rho_0 {}^e a_\rho {}^e b_\rho e^{{}^e b_\rho e_R} c_R \left(1 - \frac{\|{}^e \alpha\|}{e_R} \right) \dot{\xi} \\ &\stackrel{(15e)}{=} {}^e \dot{s}_n - \left\{ {}^e n : \sum_j {}^e c_j \left({}^e n - \left(\frac{\|{}^e \alpha_j\|}{e_{r_j}} \right)^{\chi_j} {}^e \alpha_j \right) + {}^e \rho_0 {}^e a_\rho {}^e b_\rho e^{{}^e b_\rho e_R} d_\xi e_R \right\} \dot{\xi} \\ &\stackrel{(15c, 15d, 17)}{=} {}^e \dot{s}_n - \left\{ {}^e n : d_\xi {}^e \alpha + d_\xi {}^e \rho \right\} \dot{\xi} \stackrel{(17, 15d)}{=} {}^e \dot{s}_n - {}^e h \dot{\xi} \stackrel{(18)}{=} 0. \end{aligned}$$

Hence $\lambda^- = 0$, $\lambda^+ = 1$, $\mathfrak{J}_{e_s}(x) \cap \mathcal{I}_x S = \{\mathcal{I}^+(x)\}$ and theorem 2 in [9] §10 yields uniqueness. We see that the solution curves reach S and a sliding motion occurs as long as ${}^e \dot{s}_n > 0$. The solution x cannot enter $\Omega_{e_Y}^+$. As \mathcal{I}^+ and S are smooth, x will be smooth during the sliding motion along S .

2. We consider the active loading of $S_{e_Y}^\Omega$ and $S_{e_M}^\Omega$. Here the surface of discontinuity is given by $S = S_{e_Y}^\Omega \cap S_{e_M}^\Omega$, where the normals $\nabla \varphi_{e_Y}$ and $\nabla \varphi_{e_M}$ are linearly independent (obviously due to the decoupling into the elastic and real stress space). So $S_{e_Y}^\Omega$ and $S_{e_M}^\Omega$ locally divide Ω at $x \in S$ into four quadrants, so we have $\mathfrak{J}_{e_s} = \text{conv}\{\mathcal{I}_-, \mathcal{I}_+, \mathcal{I}_-, \mathcal{I}_+\}$ with four limiting values of \mathcal{I}_{e_s} . It is straight forward to see that

$$\begin{pmatrix} 1 & 1 & 1 & 1 \\ \langle \nabla \varphi_{e_Y}, \mathcal{I}_- \rangle & \langle \nabla \varphi_{e_Y}, \mathcal{I}_+ \rangle & \langle \nabla \varphi_{e_Y}, \mathcal{I}_- \rangle & \langle \nabla \varphi_{e_Y}, \mathcal{I}_+ \rangle \\ \langle \nabla \varphi_{e_M}, \mathcal{I}_- \rangle & \langle \nabla \varphi_{e_M}, \mathcal{I}_+ \rangle & \langle \nabla \varphi_{e_M}, \mathcal{I}_- \rangle & \langle \nabla \varphi_{e_M}, \mathcal{I}_+ \rangle \end{pmatrix} \begin{pmatrix} \lambda_-^- \\ \lambda_+^+ \\ \lambda_-^- \\ \lambda_+^+ \end{pmatrix} = \begin{pmatrix} 1 \\ 0 \\ 0 \\ 0 \end{pmatrix}$$

has exactly one solution, thus $\mathfrak{J}_{e_s}(x) \cap \mathcal{I}_x S = \{\mathcal{I}_+^+(x)\}$. Here as well a sliding motion occurs, the solution can neither enter $\Omega_{e_Y}^+$ nor $\Omega_{e_M}^+$. As S is smooth and \mathcal{I}_+^+ is Lipschitz, x will be smooth during the sliding motion along S .

3. It is clear that the cases, where the solution x meets a point on $S_{e_M}^\Omega \cap \Omega_{e_Y}^-$ or $S_M^\Omega \cap \Omega_{e_Y}^-$ cannot occur. The active loading of $S_{e_Y}^\Omega$ and S_M^Ω is treated exactly in the same way as in the second step, and the active loading of $S_{e_Y}^\Omega$, $S_{e_M}^\Omega$ and S_M^Ω (the octant) is as well treated straight forwardly.

Theorem 2.6 (Local existence and uniqueness of solution) *Let $V = \mathbb{R}_s^{3 \times 3}$ or $V = \mathbb{R}_{sp}^{3 \times 3}$.*

(a) Jiang correction model. *As long as condition (30) is satisfied and none of ${}^e \alpha$ and the ${}^e \alpha_i$ passes through the origin, there exists one uniquely determined, absolutely continuous Filippov-solution of (9) under the initial values/conditions (19), if the elastic stress deviator ${}^e s$ is of class $\mathcal{C}_{pw}^1([0, T], V_d)$.*

(b) Jiang model. *As long as condition (27) is satisfied and none of α and the α_i passes through the origin, there exists one uniquely determined absolutely continuous Filippov-solution of (25) under the initial values/conditions (26), if the stress deviator s is of class $\mathcal{C}_{pw}^1([0, T], V_d)$.*

Proof: (a) 1. Assume first ${}^e \sigma \in \mathcal{C}^1([0, t_1])$. Uniqueness: See steps above. To ensure local existence by applying the first part of theorem 1 §7 in [9], we remark that

- the function $(t, x) \mapsto \mathfrak{J}_{e_s}(x)$ is set valued and upper semicontinuous (in the sense of [9], sect. 3, §5) in (t, x) . In order to verify this, see [9], lemma 3, §6 and the corollary after lemma 4.

- for all (t, x) the set $\mathcal{J}_{e_s}(x)$ is nonempty, bounded, closed and convex.
2. Induction: ${}^e\sigma \in \mathcal{C}^1([t_{n-1}, t_n])$, $0 = t_0 < t_1 < \dots < t_N = T$, $n = 1, \dots, N$.
 (b) Clear, as Jiang's constitutive model (25) is a subsystem of (9). Just drop each e . \blacksquare

2.3 A special case

If for any $i \in \{1, \dots, m\}$ the ratchetting parameter eQ_i is equal to zero, the differential equation for the partial backstress ${}^e\alpha_i$ simplifies to

$${}^e\dot{\alpha}_i \stackrel{(15c)}{=} {}^e c_i ({}^e r_i {}^e n - {}^e \alpha_i) \dot{\xi} \stackrel{(18)}{=} {}^e c_i ({}^e r_i \dot{\varepsilon}^{pl} - \dot{\xi} {}^e \alpha_i) \quad (37)$$

the right-hand side being a generalization of the backstress evolution equations of ARMSTRONG/FREDERICK [1] resp. CHABOCHE, see [4, 5, 14], since ${}^e c_i = {}^e c_i(\xi)$ is non-constant. If we insert $\dot{\varepsilon}^{pl} = \dot{\xi}({}^e s - {}^e \alpha)/{}^e \rho$, equation (37) becomes

$${}^e\dot{\alpha}_i = {}^e c_i(\xi(t)) \dot{\xi}(t) \left({}^e r_i \frac{{}^e s(t) - {}^e \alpha(t)}{{}^e \rho(t)} - {}^e \alpha_i \right) \quad (38)$$

a system of ordinary differential equations of first order. If the functions ${}^e\alpha$, ${}^e s$, ${}^e \rho$, ξ are of class \mathcal{AC} and $\|{}^e s(t) - {}^e \alpha(t)\| \leq {}^e \rho(t)$, $\dot{\xi} \geq 0$ for almost every $t \in [0, T]$, we can solve (38) by variation of constants, yielding the explicit formula

$${}^e\alpha_i(t) = \frac{1}{{}^e W_i(t)} \left\{ {}^e\alpha_i(0) + {}^e r_i \int_0^t \frac{{}^e s(\tau) - {}^e \alpha(\tau)}{{}^e \rho(\tau)} {}^e W_i(\tau) d\tau \right\} \quad (39)$$

for almost every $t \in [0, T]$, where

$${}^e W_i(t) = \exp \left(\int_0^t {}^e c_i(\xi(\tau)) \dot{\xi}(\tau) d\tau \right) = \exp ({}^e c_i \circ \xi|_0^t)$$

An analogueous equation to (38) and solution formula (39) holds of course in the real stress space too. Using (39), we can give an alternative proof of lemma 2.4.

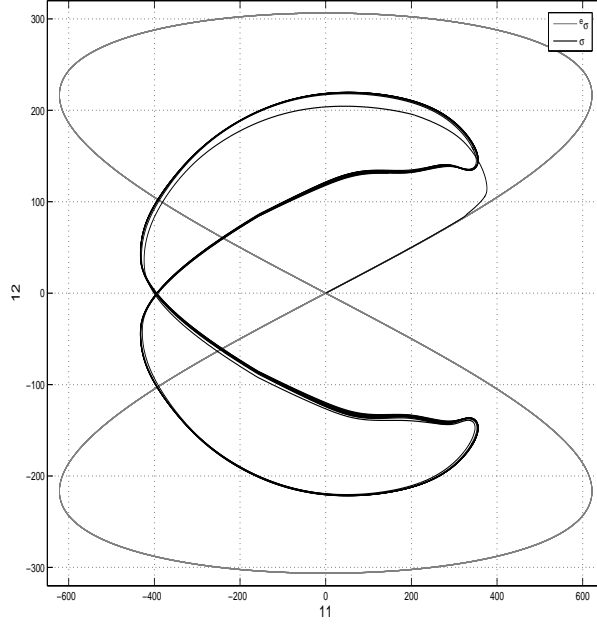
3 Numerical Implementation

Throughout this section, we are concerned with the 'notch' case (9), (11). Clearly, our algorithm is applicable to (25) as well. For implementation of \mathcal{J}_{e_s} and \mathcal{L} , we consider $\dot{y} = \mathcal{J}_{e_s}(t, y)$ in the non-redundant form, where $y \in \mathbb{R}^{3(2m+1)+3}$ where the scalar product on $V_d = \mathbb{R}_{spd}^{3 \times 3} \simeq \mathbb{R}^3$, $A \simeq (a_{11}, a_{22}, a_{12})^T$, considered as subspace of $\mathbb{R}^{3 \times 3}$, is given by

$$\langle x, y \rangle_M = x^T M y, \quad M = \begin{pmatrix} 2 & 1 & 0 \\ 1 & 2 & 0 \\ 0 & 0 & 2 \end{pmatrix}, \quad \|x\|_M^2 = \langle x, x \rangle_M \quad (x, y \in \mathbb{R}^3).$$

We consider a discrete finite sequence of given elastic stress tensors ${}^e\sigma_0, \dots, {}^e\sigma_N$ at times $t_0 = 0, \dots, t_N = T$, $N \in \mathbb{N}$ and assume ${}^e\sigma$ to be piecewise linear:

$${}^e\sigma(t) = {}^e\sigma_n + (t - t_{n-1}) \frac{\Delta {}^e\sigma_n}{\Delta t_n}, \quad \Delta {}^e\sigma_n = {}^e\sigma_n - {}^e\sigma_{n-1}, \quad \dot{\sigma}(t) = \frac{\Delta {}^e\sigma_n}{\Delta t_n} \quad (40)$$

Figure 2: Elastic stress $\epsilon\sigma$ and corrected stress σ

for $n = 1, \dots, N$ and $t \in [t_{n-1}, t_n]$. This is the usual case in engineering practice, where only such sampled data (or ‘signals’) are available. Theorem 2.6 guarantees a unique solution. Because of rate independency we may assume $\Delta t_n = t_n - t_{n-1} = 1$ and thus $T = N$. Application of dev to (40) implies

$${}^e s(t) = {}^e s_n + (t - n + 1)\Delta^e s_n, \quad \Delta^e s_n = {}^e s_n - {}^e s_{n-1}, \quad {}^e \dot{s}(t) = \Delta^e s_n \quad (41)$$

Discontinuity detection at S_{eY} . The idea is simply to reparametrize $\tau_n = t - n + 1$ and to calculate the exact intersection point ${}^e s_n^*$ of the straight arc $\{\tau_n \mapsto {}^e s_{n-1} + \tau_n \Delta^e s_n : \tau_n \in [0, \infty)\}$ with S_{eY} , whose position remains constant on $[0, \tau_n^*]$. Setting ${}^e \beta_{n-1} = {}^e s_{n-1} - {}^e \alpha_{n-1}$ we have ${}^e s_n^* = {}^e s_{n-1} + \tau_n^* \Delta^e s_n$ with

$$\tau_n^* = \frac{-\langle {}^e \beta_{n-1}, \Delta^e s_n \rangle_M + \left(\langle {}^e \beta_{n-1}, \Delta^e s_n \rangle_M^2 - \|\Delta^e s_n\|_M^2 (\|{}^e \beta_{n-1}\|_M^2 - {}^e \rho_n^2) \right)^{1/2}}{\|\Delta^e s_n\|_M^2} \quad (42)$$

if $\Delta^e s_n \neq 0$ and

$$\tau_n^* = \infty \quad (43)$$

otherwise. If $\tau_n^* \in [0, 1)$, it follows from the sliding motion reflections in section 2 that ${}^e s(\tau) \in S_{eY}(\tau)$ for $\tau \in [\tau_n^*, 1]$, otherwise ${}^e s(\tau) \in B_{e\rho(\tau)}({}^e \alpha(\tau)) = B_{e\rho(0)}({}^e \alpha(0))$ for $\tau \in [0, 1]$. This kind of front checking leads to a significant reduction of rejected steps, when using a standard ODE method with error control, see HAIRER et al. [11], ch. II.6. The discontinuities at S_{eM} and S_M are left to the step size control. Using a constant step size would yield too large errors when crossing these discontinuities.

3.1 The algorithm.

It turns the

$$\text{INPUT } {}^e\sigma_n, (n = 0, \dots, N), \quad {}^e p_l, p_l (l = 1, \dots, 7m + 6)$$

into

$$\text{OUTPUT } \sigma_n, s_n, \varepsilon_n, \varepsilon_n^{el}, \varepsilon_n^{pl}, {}^e\alpha_n^i, {}^e\alpha_n, {}^eR_n, {}^e\rho_n, \alpha_n^i, \alpha_n, R_n, \rho_n, \xi_n (n = 0, \dots, N)$$

Lower indices $*_n$ are loop indices whereas the upper indices $*^i$ enumerate the backstresses. It reads as follows

A ${}^e\sigma_0^{pl}, \xi_0, {}^e\alpha_0^i, {}^eR_0, \alpha_0^i, R_0 := \text{acc. to (19)}$

B ${}^e\alpha_0, {}^e\rho_0, \alpha_0, \rho_0, s_0 := \text{as in (12), (22)}, {}^e s_0 := \tilde{D}^e\sigma_0 \text{ as in (41)}$

C for $n := 1, \dots, N$

D ${}^e s_n := \tilde{D}^e\sigma_n, \Delta^e s_n := {}^e s_n - {}^e s_{n-1} \text{ as in (41)}$

E $\tau_n^* := \text{as in (42), (43)}$

F if $0 \leq \tau_n^* < 1$

G ${}^e s_n^* := {}^e s_{n-1} + \tau_n^* \Delta^e s_n, \Delta^e s_n^* := {}^e s_n - {}^e s_n^*$

H ${}^e\varepsilon_n^{pl}, \xi_n, {}^e\alpha_n^i, {}^eR_n, \alpha_n^i, R_n := \text{DOPRI5-solution at } \tau = 1 \text{ of } \dot{y} = \mathcal{J}_{\varepsilon_s}(\tau, y) \text{ over } \tau \in [0, 1]$
with initial values ${}^e\varepsilon_{n-1}^{pl}, \xi_{n-1}, {}^e\alpha_{n-1}^i, {}^eR_{n-1}, \alpha_{n-1}^i, R_{n-1}$
and external input ${}^e s(\tau) = {}^e s_n^* + \tau \Delta^e s_n^*, {}^e \dot{s}(\tau) = \Delta^e s_n^*$

I else

J ${}^e\varepsilon_n^{pl}, \xi_n, {}^e\alpha_n^i, {}^eR_n, \alpha_n^i, R_n := {}^e\varepsilon_{n-1}^{pl}, \xi_{n-1}, {}^e\alpha_{n-1}^i, {}^eR_{n-1}, \alpha_{n-1}^i, R_{n-1} \text{ acc. to (14)}$

K ${}^e\alpha_n, {}^e\rho_n, \alpha_n, \rho_n, s_n := \text{as in (12), (22)}$

L $\sigma_n := \tilde{D}^{-1} s_n, \varepsilon_n^{el} := \tilde{C}^{-1} \sigma_n, \varepsilon_n := \varepsilon_n^{el} + \check{D}^{-1} \varepsilon_n^{pl} \text{ as in (23)}$

Here

$$\tilde{D} = \begin{pmatrix} 2/3 & -1/3 & 0 \\ -1/3 & 2/3 & 0 \\ 0 & 0 & 1 \end{pmatrix}, \quad \tilde{C}^{-1} = \left(\begin{array}{cc|c} 1/E & -\nu/E & 0 \\ -\nu/E & 1/E & 0 \\ -\nu/E & -\nu/E & 0 \end{array} \right), \quad \check{D}^{-1} = \left(\begin{array}{cc|c} 1 & 0 & 0 \\ 0 & 1 & 0 \\ -1 & -1 & 0 \\ \hline 0 & 0 & 1 \end{array} \right).$$

That way, we push the trivial integration (14) into an *outer* loop (stepsize $\Delta t_n = 1$, rate-independency!). For the *inner* loop (step H, variable step size h) we have tested all methods with step size control contained in SHAMPINE/REICHELDT [20], among which the Runge-Kutta method of DORMAND/PRINCE – see RK4(5)7M in [6], DOPRI5 in [11], sect. II.5 or [20], sect. 5 – has turned out to be the fastest. The initial step size and the steps size control has been performed as in [11], sect. II.4.

3.2 The butterfly test.

We consider ${}^e\sigma(t) = L_{11}(t){}^e\sigma_{11} + L_{22}(t){}^e\sigma_{22} + L_{12}(t){}^e\sigma_{12}$ as in (2), in which ${}^e\sigma_{11} = (1, 0, 0)^T$, ${}^e\sigma_{22} = (0, 1, 0)^T$, ${}^e\sigma_{12} = (0, 0, 1)^T$. All parameters for the steel S460N and an appropriate notch of an axis are taken from [12] and [13].

j	${}^e r_j$	${}^e c_j^\infty$	${}^e a_j^{(1)}$	${}^e b_j^{(1)}$	${}^e a_j^{(2)}$	${}^e b_j^{(2)}$	${}^e Q_j$	${}^e \rho_0$	2.02E^{+2}
1	9.5E^1	1.10E^3	-4.3E^{-2}	7.74E^1	-4.80E^{-2}	7.0E^{-3}	1.4E^{+0}	${}^e a_\rho$	-2.88E^{-1}
2	7.0E^1	3.53E^2	-6.8E^{-2}	4.44E^1	-1.09E^{-1}	1.5E^{-2}	1.4E^{+0}	${}^e b_\rho$	-6.16E^{-3}
3	1.0E^2	1.79E^2	-7.1E^{-2}	3.46E^1	-9.40E^{-2}	2.0E^{-2}	1.4E^{+0}	${}^e a_\chi$	2.85E^{-1}
4	1.7E^2	7.20E^1	-8.0E^{-2}	3.00E^1	-1.32E^{-1}	2.0E^{-2}	1.4E^{+0}	${}^e b_\chi$	-6.45E^{-3}
5	8.1E^2	3.71E^1	-7.0E^{-2}	2.70E^1	-7.60E^{-2}	3.5E^{-2}	1.4E^{+0}	${}^e c_R$	1.00E^{+2}
j	r_j	c_j^∞	a_j^1	b_j^1	a_j^2	b_j^2	Q_j	ρ_0	2.11E^{+2}
1	9.0E^1	1.16E^3	-2.4E^{-1}	1.88E^1	2.95E^{-1}	1.7E^{+0}	1.0E^{-2}	a_ρ	-3.20E^{-1}
2	5.0E^1	3.58E^2	-4.0E^{-1}	1.88E^1	3.86E^{-1}	3.0E^{+0}	1.0E^{-2}	b_ρ	-7.60E^{-3}
3	4.0E^1	1.86E^2	-2.0E^{-1}	3.00E^1	-3.00E^{-1}	2.0E^{-2}	1.0E^{-2}	a_χ	5.00E^{+4}
4	4.0E^1	7.10E^1	-3.0E^{-1}	2.50E^1	-3.50E^{-1}	2.0E^{-2}	1.0E^{-2}	b_χ	-2.60E^{-2}
5	7.0E^1	3.74E^1	-2.5E^{-1}	2.00E^1	-6.00E^{-1}	3.0E^{-2}	1.0E^{-2}	c_R	1.00E^{+2}

and $E = 2.085\text{E}^5$, $\nu = 3.0\text{E}^{-1}$. Here $m = 5$, so altogether, the number of independent differential equations is 36, the number of parameters 84. All quantities of physical dimension ‘stress’ are measured in MPa.

You should monitor, that sufficient condition (30) is not violated during integration. The critical value at its right hand side is ${}^e\rho_0 {}^e a_\rho {}^e b_\rho {}^e c_R \leq 35.75$. Likewise, you should monitor that $({}^e R(t), R(t))$ lies in the *correction region* $\{({}^e R, R) \in (0, \infty)^2 : {}^e f({}^e R) = {}^e \rho > \rho = f(R)\}$.

As proposed in [12], we consider the smooth periodic input

$$L_{11}(t) = 621.63 \sin(2\omega t), \quad L_{22}(t) = 0, \quad L_{12}(t) = 306.38 \sin(\omega t), \quad \omega = 2\pi/8 \quad (44)$$

over the time interval $[0, T]$ with $T = 80$, i.e. 10 cycles. (44) is obtained from the original one by a rotation of the coordinate system. The results are depicted in figure 2.

We compare the ‘exact’ solution (DOPRI5 algorithm with smooth input and relative accuracy $\delta = 10^{-9}$) with our solution with sampled input $N = 80 \cdot 4^2$ and relative accuracy $\delta = 10^{-3}$. The relative error is depicted in figure 3. The largest peaks occur, where σ is very close to zero.

But the reduction of running time is remarkable, as seen in figure 4, where we compare DOPRI5-Algorithm with smooth input and various relative accuracies δ with the solution of our algorithm with sampled input data: $k \in \{0, \dots, 5\}$, $\Delta t_n = 4^{-k}$, $N = 80 \cdot 4^k$ sample intervals. Of course, the falsification of the input loading path is of order $\mathcal{O}(\Delta t_n)$.

All loading paths in [12] have been tested as benchmark tests with similar results concerning speed and accuracy.

4 Conclusion

We have proven local existence and uniqueness of solution Jiang constitutive model of elasto-plasticity. A proper formulation for a stress spaced stress-correction model has been given.

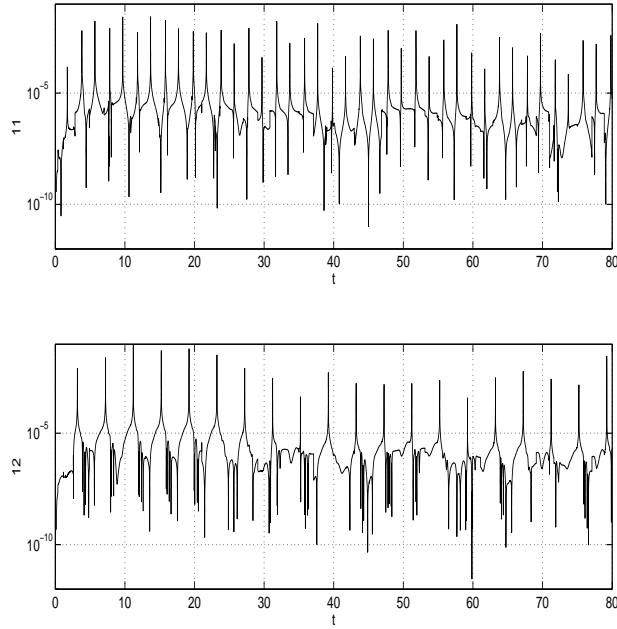


Figure 3: Relative error

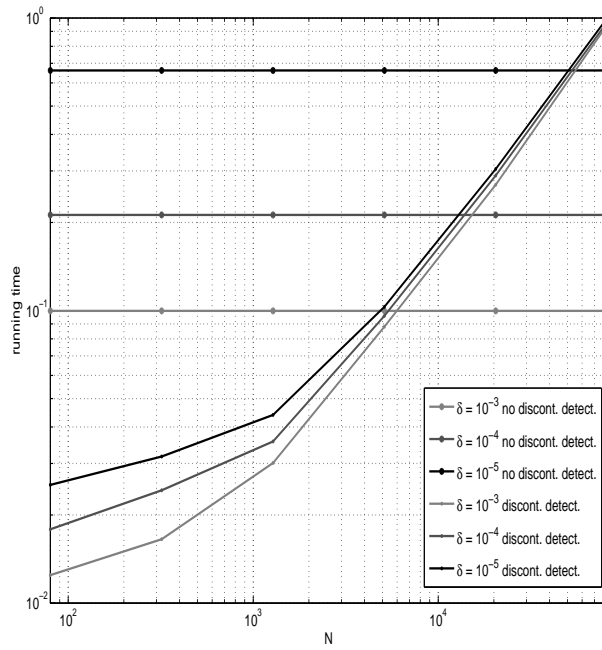


Figure 4: Running times with(out) discontinuity detection

Through the simultaneity coupling inherent in the model, we have been able to implement a solution algorithm which is much faster than existing ones. Through a discontinuity detection method for sampled input data further improvement of performance has been achieved.

Parameter identification. The quality of results of our model is comparable with approaches using an incremental form of NEUBER's formula, where no elastic parameters are needed, see GLINKA et al. [10].

For practice, finding appropriate ϵp_l in our model may be a problem. But the advantage of our correction scheme is that we have the freedom of adjusting the ϵp_l – or even the p_l – in order to optimally fit measurements or nonlinear PDE results (with Jiang's constitutive material law).

A derivation of elastic parameters ϵp_l from uniaxial equivalent load-notch strain curves can be found in HERTEL [12], sect. 4.4, automatic optimization of the p_l , ϵp_l in LANG et al. [17].

Future tasks. Numerical challenges for the future are a further reduction of rejected steps, maybe by detecting the discontinuities at S_{eM} and S_M with Runge-Kutta interpolation/dense output methods of ENRIGHT/JACKSON [7, 8].

An open question is, if it is possible to generalize our theoretical result to inputs σ resp. ε of certain subsets \mathcal{S} , $\mathcal{E} \subseteq \mathcal{AC}([0, T], \mathbb{R}_s^{3 \times 3})$ in order to have proper 'Jiang'-operators

$$\mathcal{F} : \mathcal{S} \rightarrow \mathcal{E}, \sigma \mapsto \varepsilon = \mathcal{F}[\sigma], \quad \mathcal{F}^{-1} : \mathcal{E} \rightarrow \mathcal{S}, \varepsilon \mapsto \sigma = \mathcal{F}^{-1}[\varepsilon]$$

turning stress into strain and vice versa.

Acknowledgements. Thanks to the DFG and the GKMP Kaiserslautern for the financial support and to Olaf Hertel (TU Darmstadt, dept. of material science) for his kind provision of data.

References

- [1] ARMSTRONG P. J., FREDERICK C. O.: *A mathematical representation of the multiaxial Bauschinger effect*. CEGB, report RD/B/N 731, 1966.
- [2] BROKATE M.: *Elastoplastic constitutive laws of nonlinear kinematic hardening type*. Pitman research notes in mathematics series, Vol. 377, pp. 238-272, 1998.
- [3] BROKATE M., KREJCI P.: *On the wellposedness of the Chaboche model*. International series of numerical mathematics, Vol. 126, pp. 67-79, 1998.
- [4] BROKATE M., KREJCI P.: *Wellposedness of kinematic hardening models in elastoplasticity*. Mathematical modelling and numerical analysis, Vol. 32, No. 32, pp. 177-209, 1998.
- [5] CHABOCHE J.-L.: *On some modifications of kinematic hardening to improve the description of ratchetting*. International journal of plasticity, Vol. 7, pp. 661-678, 1991.
- [6] DORMAND J. R., PRINCE P.J.: *A family of embedded Runge-Kutta formulae*. Journal of computational and applied mathematics, Vol. 6, No. 1, pp. 19-26, 1980.
- [7] ENRIGHT W. H., JACKSON K. R.: *Interpolants for Runge-Kutta formulas*. ACM transactions on mathematical software, Vol. 12, No. 3, pp. 193-218, 1986.
- [8] ENRIGHT W. H., JACKSON K. R.: *Effective solution of discontinuous IVPs using a Runge-Kutta formula pair with interpolants*. Applied mathematics and computation, Vol. 27, pp. 313-335, 1988.

- [9] FILIPPOV A. F.: *Differential equations with discontinuous righthand sides*. Kluwer Academic Publishers, 1988.
- [10] GLINKA G., BUCYNSKI A., RUGGERI A.: *Elastic-plastic stress-strain analysis of notches under non-proportional loading paths*. Archives of mechanics, Vol. 52, No. 4-5, pp. 589-607, 2000.
- [11] HAIRER E., NOERSET S.P., WANNER G.: *Solving ordinary differential equations I*. Springer-Verlag Berlin Heidelberg, 1993.
- [12] HERTEL O.: *Weiterentwicklung und Verifizierung eines Näherungsverfahrens zur Berechnung von Kerbbeanspruchungen bei mehrachsiger nichtproportionaler Schwingbelastung*. Diplomarbeit, Bauhaus-Universität Weimar, 2003.
- [13] HOFFMEYER J., DÖRING R., SCHLIEBNER R., VORMWALD M., SEEGER T.: *Lebensdauervorhersage für mehrachsige nichtproportional schwingbeanspruchte Werkstoffe mit Hilfe des Kurzrissfortschritt-konzeptes*. FD-2/2000, FG Werkstoffmechanik, Technische Universität Darmstadt, 2000.
- [14] JIANG Y., SEHITOGLU H.: *Modeling of cyclic ratchetting plasticity, part I: Development of constitutive relations*. Transactions of the ASME, Vol. 63, pp. 720-725, 1996.
- [15] JIANG Y., SEHITOGLU H.: *Modeling of cyclic ratchetting plasticity, part II: Comparison of model simulations with experiments*. Transactions of the ASME, Vol. 63, pp. 726-733, 1996.
- [16] KÖTTGEN V. B., BARKEY M. E., SOCIE D. F.: *Pseudo stress and pseudo strain based approaches to multiaxial notch analysis*. Fatigue and fracture of engineering materials and structures, Vol. 18, No. 9, pp. 981-1006, 1995.
- [17] LANG H., PINNAU R., DRESSLER K.: *Parameter optimization for a stress-strain correction scheme*. AGTM report, TU Kaiserslautern, No. 264, 2005;
- [18] MROZ Z.: *An attempt to describe the behaviour of metals under cyclic loads using a more general workhardening model*. Acta mechanica, Vol. 7, pp. 199-212, 1969.
- [19] NEUBER H.: *Theory of stress concentration for shear-strained prismatical bodies with arbitrary nonlinear stress-strain law*. Journal of applied mechanics, Transactions of the ASME, Vol. E28, pp. 544-550, 1961.
- [20] SHAMPINE L. F., REICHEL T. M. W.: *The Matlab ODE suite*. SIAM journal on scientific computing, Vol. 18, No. 1, 1997.